AD-A251 057

②

TECHNICAL REPORT NO. 44

The Thermal Dissociation of Decaborane on Si(111)-(7x7) and

Doping Effects in the Near Surface Region

by

P.J. Chen, M.L. Colaianni and J.T. Yates, Jr.

Submitted to

DTIC
S ELECTE D
JUN 03 1992
A

J. Appl. Phys.

Surface Science Center
Department of Chemistry
University of Pittsburgh
Pittsburgh, PA 15260

May 1, 1992

92-14492

92 6 01 155

MASTER COPY   —   FOR REPRODUCTION PURPOSES

REPORT DOCUMENTATION PAGE		READ INSTRUCTIONS BEFORE COMPLETING FORM
1. REPORT NUMBER 44	**2. GOVT ACCESSION NO.**	**3. RECIPIENT'S CATALOG NUMBER**
4. TITLE (and Subtitle) The Thermal Dissociation of Decaborane on Si(111) -(7x7) and Doping Effects in the Near Surface Region		**5. TYPE OF REPORT & PERIOD COVERED** Preprint
		6. PERFORMING ORG. REPORT NUMBER
7. AUTHOR(s) P.J. Chen, M.L. Colaianni and J.T. Yates, Jr.		**8. CONTRACT OR GRANT NUMBER(s)**
9. PERFORMING ORGANIZATION NAME AND ADDRESS Surface Science Center Department of Chemistry University of Pittsburgh, Pittsburgh, PA 15260		**10. PROGRAM ELEMENT, PROJECT, TASK AREA & WORK UNIT NUMBERS**
11. CONTROLLING OFFICE NAME AND ADDRESS		**12. REPORT DATE** May 1, 1992
		13. NUMBER OF PAGES 27
14. MONITORING AGENCY NAME & ADDRESS(If different from Controlling Office)		**15. SECURITY CLASS. (of this report)** Unclassified
		15a. DECLASSIFICATION/DOWNGRADING SCHEDULE

16. DISTRIBUTION STATEMENT (of this Report)

17. DISTRIBUTION STATEMENT (of the abstract entered in Block 20, if different from Report)

18. SUPPLEMENTARY NOTES

boron   decaborane
silicon
silicon (111)

19. KEY WORDS (Continue on reverse side if necessary and identify by block number)

20. ABSTRACT (Continue

The thermal decomposition of decaborane ($B_{10}H_{14}$) and its doping effects on Si(111)-(7x7) has been investigated by surface spectroscopies. Upon adsorption between 100-300 K, molecular decaborane was identified on the surface by HREELS by the absence of Si-H surface species production. The thermal decomposition of adsorbed decaborane molecules involves a preferential removal of hydrogen from the weaker B-H-B linkage. H_2 thermal desorption was observed to cover a wide temperature range between 300-900 K. Clean boron deposition on the surface was achieved at ~900 K. Upon heating to ~1275 K, extensive boron diffusion into bulk silicon produced a highly B-doped region below the surface (~10^3 Å) with a carrier hole concentration on the order of ~10^{19} cm^{-3} depending upon the initial surface boron coverage and annealing conditions. The surface adopted a ($\sqrt{3} \times \sqrt{3}$)R30° reconstruction with a nominal 1/3 ML boron occupying subsurface substitutional sites. Both the localized B-Si vibration and carrier surface plasmon excitation were observed by HREELS at 100 K.

DD FORM 1473
1 JAN 73

The Thermal Dissociation of Decaborane on Si(111)-(7x7) and Doping Effects in the Near Surface Region

P. J. Chen[#], M. L. Colaianni and J. T. Yates, Jr.

Surface Science Center
Department of Chemistry
University of Pittsburgh
Pittsburgh, PA 15260

[#]Department of Physics, University of Pittsburgh, Pittsburgh,
PA 15260

The Thermal Dissociation of Decaborane on Si(111)-(7x7) and Doping Effects in the Near Surface Region

P. J. Chen[#], M. L. Colaianni and J. T. Yates, Jr.

Surface Science Center
Department of Chemistry
University of Pittsburgh
Pittsburgh, PA 15260

Abstract

The thermal decomposition of decaborane ($B_{10}H_{14}$) and its doping effects on Si(111)-(7x7) has been investigated by surface spectroscopies. Upon adsorption between 100-300 K, molecular decaborane was identified on the surface by HREELS by the absence of Si-H surface species production. The thermal decomposition of adsorbed decaborane molecules involves a preferential removal of hydrogen from the weaker B-H-B linkage. H_2 thermal desorption was observed to cover a wide temperature range between 300-900 K. Clean boron deposition on the surface was achieved at ~900 K. Upon heating to ~1275 K, extensive boron diffusion into bulk silicon produced a highly B-doped region below the surface (~10^3 Å) with a carrier hole concentration on the order of ~10^{19} cm^{-3} depending upon the initial surface boron coverage and annealing conditions. The surface adopted a ($\sqrt{3}$x$\sqrt{3}$)R30° reconstruction with a nominal 1/3 ML boron occupying subsurface substitutional sites. Both the localized B-Si vibration and carrier surface plasmon excitation were observed by HREELS at 100 K.

2

I. INTRODUCTION

Boron has been a conventional dopant in group-IV elements to yield p-type semiconducting material. Boron on silicon has received much attention recently due to the surface reconstruction boron induces [1-3] and to a series of novel properties associated with the modification of the silicon surface. Among these are: (1) the quenching of surface chemistry on Si(111) by subsurface boron doping [4-6]; and (2) the δ-doping of silicon by boron and its potential device applications [7-10]. Other technological interests involving boron include the growth of insulating boron nitride thin-films [11,12] as hard protective coatings that possess excellent resistivity and dielectric properties, and the growth and application of boron carbide as a refractory semiconductor[12,13].

Boron hydrides, or boranes, make excellent molecular precursors for boron deposition on silicon surfaces at low temperatures. However, the simplest boron hydride, diborane (B_2H_6), has been shown to have only a negligible sticking coefficient on Si(100) at room temperature [14]. The use of the more complex pentaborane (B_5H_9) and decaborane ($B_{10}H_{14}$) as molecular sources of boron, on the other hand, has been successful [3,11-13]. Aside from the conventional approach of thermally dissociating boranes to yield boron deposition, alternatives such as photon [12,13] and electron-induced [15] dissociation have also been pursued with success. In view of these developments, it is important to gain a systematic surface chemical understanding of $B_{10}H_{14}$ adsorption, dissociation, and the subsequent transport of

3

boron in the near surface region of silicon crystals. This work addresses these issues by applying surface sensitive techniques to investigate the thermal behavior of $B_{10}H_{14}$ on the Si(111)-(7x7) surface.

II. EXPERIMENTAL

The experiments were performed in a stainless-steel UHV system with a typical base pressure near $1x10^{-10}$ mbar. The UHV system is equipped with the following apparatus: a single-pass cylindrical mirror analyzer (CMA) Auger electron spectrometer; a home-built low-energy electron diffraction (LEED) system; a shielded quadrupole mass spectrometer (QMS) designed for line-of-sight temperature programmed desorption (TPD) studies; and a high resolution electron energy loss spectrometer for surface vibrational studies. The silicon crystals used in this study were p-type boron-doped (5-10 $\Omega \cdot cm$ nominal resistivity), Czochralski-grown wafers of dimension 13x13x1.5 mm. They were commercially polished and oriented to within 0.5° of the <111> direction. Prior to introduction into the UHV system, the crystal was cleaned by the extended RCA wet chemical process to remove possible imbedded metal impurities from the crystal edges due to cutting. The crystal was then mounted onto a liquid N_2-cooled sample manipulator in the UHV system [16]. Direct resistive heating was employed to give control of the crystal temperature in the range 100 to 1200 K, as measured with an imbedded type-E (chromel-constantan) thermocouple which is shielded from the silicon by a tantalum foil envelope. The in situ

cleaning of the crystal was routinely carried out by cycles of Ar^+ ion sputtering at 2.5 keV and subsequent thermal annealing at 1173 K. The surface structure and cleanliness were determined by low energy electron diffraction and Auger spectroscopy, respectively. Decaborane ($B_{10}H_{14}$, Aldrich) was introduced into the UHV system through a metal leak valve. The mass spectrometer cracking pattern [17] was used to identify gas phase decaborane and to verify its purity. The Si(111) surface was exposed to the decaborane background pressure for dosing. Due to the high molecular weight of $B_{10}H_{14}$, the pump-down time of the UHV system was rather long (10^2-10^3 sec) after closing the leak valve. Therefore, only an approximate exposure can be given based on the time-integrated pressure reading from an uncorrected Bayard-Alpert ionization gauge in the units of Langmuirs (1 L = 10^{-6} Torr sec). The HREEL measurements were made at a primary electron energy E_p=3.2-6.1 eV and a resolution of ~100 cm^{-1}. All specular HREELS measurements were made at 60° angle of incidence.

III. RESULTS

3.1. Adsorption of $B_{10}H_{14}$ on Si(111)-(7x7) between 100 and 300 K

Auger spectroscopy measurements indicate that the adsorption of decaborane occurs readily on a clean Si(111) surface with high sticking efficiency in the temperature range of 100 to 300 K. A continuous uptake of boron with decaborane exposure is indicative of multilayer condensation on the surface. The HREEL spectra from

such condensed decaborane overlayers at 100 K are shown in Figure 1a for increasing surface coverages as indicated by the B(179 eV)/Si(92 eV) Auger ratio. Based on the measured Auger ratio corresponding to 1/3 ML (1 ML= 7.8×10^{14} cm^{-2}) of subsurface boron (see Section 3.3) and the information on electron escape depth in Si [18], the surface coverages of the $B_{10}H_{14}$ overlayer on Si(111) in Figure 1a are determined to be (as $B_{10}H_{14}$ molecules) 0.06, 0.35 and ~6.0 ML respectively. The HREEL spectrum taken at 0.06 ML coverage (submonolayer regime) is of particular importance since it confirms the non-dissociative nature of $B_{10}H_{14}$ adsorption by the absence of the Si-H stretching mode near 2100 cm^{-1}. All the spectra show vibrational bands characteristic of the decaborane molecule. Despite the large number of vibrational normal modes associated with this complex molecule and the limited spectral resolution of HREELS, the principal vibrational bands measured in HREELS correlate fairly well with the infrared absorption measurements of decaborane (Figure 1b). The assignments of the major vibrational bands based on infrared measurements [19,20] are summarized in Table I. Considering the molecular structure of decaborane (Figure 2), two major spectral regions are of particular importance to us: (1) the vibrational modes belonging to bridge-bonded hydrogen, B-H-B, between 1500 - 2000 cm^{-1} and (2) the vibration of terminal B-H at ~2600 cm^{-1}. The purpose of the HREELS measurements here is to establish the molecular identity of adsorbed decaborane through the 'fingerprint' vibrational spectrum rather than the analysis and assignment of all the vibrational modes. Our determination that molecular adsorption occurs agrees

6

very well with recent studies of the same system by photoemission at 100 K [13] and by STM at room temperature [15].

3.2. Thermal Behavior of the Boron-containing Overlayer: Dissociation and Desorption

Upon heating the decaborane overlayer above 300 K, a continuous evolution of $H_2(g)$ is observed in a temperature programmed desorption measurement (Figure 3). The shielded QMS with line-of-sight detection capability was employed here to carry out desorption measurements with the Si(111) crystal positioned ~ 4 mm in front of a 3 mm diameter sampling aperture. The H_2 production, superimposed on a sloping background, is caused by the thermal dissociation of decaborane molecules; the desorption of decaborane does not contribute to the m/e=2 signal based on its mass-spectral cracking pattern [17]. Compared to the H_2 desorption state associated, for example, with the thermal decomposition of simple hydride molecules such as NH_3 [16] or PH_3 [21] on Si(111), the H_2 desorption feature arising from the $B_{10}H_{14}$ overlayer spans a much wider temperature range (300-900 K). Almost no intensity is observed in the Si-H stretching region (~ 2100 cm^{-1}) by HREELS throughout the decomposition temperature range (Figure 4). The HREEL spectrum taken after heating to 700 K clearly shows modifications to the decaborane vibrational features, especially a preferential intensity reduction in the frequency region of the bridge-bonded hydrogen, B-H-B, entity (1500-2000 cm^{-1}). The strong terminal B-H stretching mode persists up to a temperature of 900 K.

All these observations can be rationalized in terms of thermal fragmentation of $B_{10}H_{14}$.

3.3. Bulk Boron Diffusion and Formation of an Ordered Surface Structure

Both TPD and HREELS indicate that, by 900 K the thermal dissociation of decaborane is complete (Figures 3 and 4). Based upon the low boron diffusion coefficient in bulk Si at this temperature [22], it can be concluded that an atomically clean boron layer is left on the surface with very little boron diffusion into the bulk of Si(111). Such a "boron covered" Si(111) surface is disordered, as indicated by the absence of any observable LEED pattern. This also agrees with STM studies of the same system [3,4].

The formation of an ordered $(\sqrt{3}x\sqrt{3})R30°$ surface reconstruction requires heating the boron-covered Si(111) surface to at least 1150 K for an extended period of time. Most of the well-ordered $(\sqrt{3}x\sqrt{3})R30°$ surfaces studied here were consistently produced by raising the crystal temperature to ~1300 K for 1-2 minutes and then annealing at 1200 K for 5-10 minutes. On all the $(\sqrt{3}x\sqrt{3})R30°$ surfaces produced by this procedure, the B(179 eV)/Si(92 eV) Auger ratio reaches a value of 0.015 ± 0.003. This value is associated with the presence of 1/3 ML B atoms under the Si-bilayer (Figure 5a). Escape depth arguments predict that 1 ML of B on a Si(111) surface would provide a B(179 eV)/Si(92 eV) ratio of 0.078, and this value is used to estimate decaborane coverage (Figure 1).

8

For the Si(111)-B($\sqrt{3}$x$\sqrt{3}$)R30° surface, rather detailed surface atomic and electronic structure characterizations already exist in the literature [1-3]. In short, the boron-stablized structure consists of surface Si atoms in the triply coordinated T_4 (adatom) site, with the B atoms occupying the energetically favorable subsurface S_5 site in the first Si bilayer (Figure 5a). The spectroscopic changes observed in HREELS will be further discussed in Section 4.2.

VI. DISCUSSION

4.1. Decaborane Dissociation Pathways

The thermal decomposition of $B_{10}H_{14}$ on Si(111) is unlike the decomposition of simple hydride molecules. The simple hydrides involve an intermediate step of Si hydride formation prior to H_2 desorption [16,21]. Decaborane decomposition does not undergo the same step forming a silicon hydride surface intermediate. This may be due to the overwhelming number of H atoms in a decaborane molecule leading to H_2 formation at boron sites; alternatively there may be a limited number of Si sites on the surface. This interpretation is based on the fact that very little intensity is observed in the Si-H stretching region by HREELS throughout the decomposition temperature. Thermal desorption measurements of H_2 evolution in a wide temperature range (Figure 3), especially at temperatures far below the normal SiH_x (x=1,2) desorption threshold, suggest that H atoms are removed as H_2 from adsorbed

9

decaborane in the decomposition process. The dehydrogenation most likely starts by the removal of bridge-bonded H atoms in the weaker B-H-B linkages, as suggested by the HREELS observation of a preferential intensity reduction in the bridged-H vibrational modes.

4.2. Bulk Doping Effects During the Formation of $(\sqrt{3}\times\sqrt{3})R30°$ Structure

At 1200 K, as the boron atoms thermally diffuse into the near surface region of bulk silicon, they become electrically active bulk acceptors. Mobile free-carrier holes are produced in the valence band of bulk silicon by the presence of boron acceptors even at 100 K. HREELS is proven to be a very valuable technique capable of monitoring both the localized B-Si bond formation and the effects of boron doping, since the low energy electrons, in addition to interacting with the dipole active vibrational modes, also interact strongly with the wave-field above the surface set up by the collective electronic excitation of free-carriers in the medium [23,24]. This is clearly shown by the spectral changes between (c) and (d) in Figure 4 following 900-1200 K heating. Here the broad energy-loss feature below 1500 cm^{-1}, arising from surface hole-plasmon excitation, starts to dominate the energy-loss spectrum.

After additional annealing at 1200 K, a typical HREEL spectrum from a well-ordered Si(111)-B$(\sqrt{3}\times\sqrt{3})R30°$ surface is shown in Figure 5b. The vibration of the localized B-Si bond in the $(\sqrt{3}\times\sqrt{3})R30°$

structure was first characterized by Rowe and coworkers [25] in a HREELS study. Their measurements showed a B-Si optical phonon mode at 835 cm^{-1} for ^{10}B, which was attributed to the stretching or breathing motion of ^{10}B in a Si matrix. A slight complication here is the presence of two boron isotopes ^{10}B and ^{11}B in our source compound $B_{10}H_{14}$. The predominant contribution, however, comes from ^{11}B (~80%). Based on the work of Rowe et. al. [25] and the results of their additional isotopic substitution studies [26], we identify the sharp energy-loss feature at 770 cm^{-1} as the ^{11}B-Si optical phonon mode ν(B-Si). Unlike the optical phonon, or the Fuchs-Kliewer modes in a polar semiconductors, this B-Si optical phonon has vibrational amplitudes strictly localized in the top 3 atomic layers and should be decoupled from the carrier surface plasmon. This is verified experimentally (data not shown) by the observation of a constant ν(B-Si) frequency unaffected by varying bulk carrier concentration levels in the near surface region.

Due to the intrinsic low mobility of free-carrier holes in p-type silicon at such a high doping level, the damping of the surface hole-plasmon is strong. As a result, the surface plasmon loss peak appears very broad. Meng et. al. recently conducted a detailed HREELS study of surface hole-plasmon excitation in highly doped p-type GaAs [24]. They pointed out that, because of the high damping and the kinematic effect involved in HREELS, it is necessary to use both the observed energy loss peak position, ω_{pp}, and a proper damping factor, Γ, in order to correctly deduce the surface hole-plasmon energy, ω_{sp}. Following the formalism outlined

in Ref.23 in a simple Drude model, $\omega_{sp} = \left(\omega_{pp}^2 + \frac{\Gamma^2}{2} \right)^{1/2} = 707$ cm^{-1} for $\omega_{pp} = 505$ cm^{-1} and $\Gamma = 700$ cm^{-1}, from which an effective carrier (hole) concentration $n_h = 2 \times 10^{19}$ cm^{-3} is obtained. Compared to the initial low doping level of the Si crystal, this high carrier concentration is a direct result of boron diffusion into the near surface region of bulk silicon, as can be expected from the high diffusivity of boron at the 1200-1300 K annealing temperature [27].

We consider the hole concentration, n_h, to be an effective or average value defined within the HREELS sampling depth. Under the experimental conditions that only small momentum transfer is involved in the inelastic scattering process, i.e. on-specular geometry and $\hbar\omega \ll E_0$, the effective sampling depth, d_{eff}, given by the dipole scattering theory [23] is $d_{eff} \approx 1/k_0 (2E_0/\hbar\omega)$, where E_0 is the electron energy and k_0 the wavevector. Applying this to the surface hole-plasmon loss in Figure 5b, a value of $d_{eff} \sim 110$ Å is obtained. This is the length scale over which the carrier concentration, n_h, is probed and averaged by HREELS. In a separate publication [28], we will further explore the possibility of utilizing HREELS measurements to extract integrated carrier depth profile information in the near surface region of Si(111).

4.3. The ($\sqrt{3}$x$\sqrt{3}$)R30° Structure and the δ-doping of Si

The ordered ($\sqrt{3}$x$\sqrt{3}$)R30° surface structure forms the basis of the "δ-doping" of Si(111). By depositing additional silicon on top of this structure, a highly boron-doped internal layer (1/3

monolayer or 7×10^{21} cm^{-3}) can be confined to the atomic-dimension in thickness [7-10]. But because a high temperature is necessary to produce the well-ordered $(\sqrt{3} \times \sqrt{3})$R30° surface structure in the first place, the thermal diffusion of boron into bulk silicon thus imposes a practical limit on the sharpness of the boron δ-doped layer. The average concentration of boron in the near surface region ($\sim 10^3$ Å) can reach as high as 10^{19}-10^{20} cm^{-3}, as deduced from the HREELS measurements of the average carrier hole concentration. This doping level represents the limitation of methods that rely on high temperature annealing to form the ordered subsurface boron structure.

Another related issue regarding the formation of Si(111)-B$(\sqrt{3} \times \sqrt{3})$R30° structure is the deviation of the subsurface boron concentration from the nominal value of 1/3 monolayer. A few initial STM studies [2-4] on boron-modified Si(111)-$(\sqrt{3} \times \sqrt{3})$R30° surfaces consistently showed that the surfaces under study were more or less boron deficient, depending on the methods of introducing boron and surface preparation. Based upon our own chemisorption/desorption yield measurements on the Si(111)-B$(\sqrt{3} \times \sqrt{3})$ surface [5,29], it is estimated that there are typically 12-20 % chemically active Si sites present on surface. Since the presence of subsurface boron in substitutional S$_5$ sites is known to suppress Si surface chemistry, the presence of chemically active Si surface sites is most likely due to the absence of these subsurface boron atoms. This boron-deficient surface condition can be improved to a certain extent by multiple decaborane adsorption/annealing cycles.

From a practical point of view, thermally decomposing adsorbed

$B_{10}H_{14}$ provides a feasible low-temperature method for clean boron deposition that has certain advantages over the traditional high-temperature Knudsen cell. It is clear the boron diffusion during the high temperature annealing is still a major obstacle to overcome since it degrades the spatial confinement of the dopant layer and prevents the formation of a truely δ-doped region. Further improvement in preparation conditions after boron deposition is necessary in order to achieve a well-ordered ($\sqrt{3}\times\sqrt{3}$) subsurface boron-doped layer while confining bulk boron diffusion.

V. CONCLUSIONS

In summary, we have investigated the adsorption and thermal dissociation of decaborane ($B_{10}H_{14}$) on Si(111)-(7x7). The following results have been obtained:

(1) The adsorption of decaborane is predominantly molecular below 300 K and occurs with high sticking efficiency.

(2) Si-H bonds do not form during $B_{10}H_{14}$ decomposition on the surface.

(3) Thermal dissociation of decaborane and desorption of hydrogen occur in a wide temperature range (300-900 K), leaving a clean boron layer deposited on the surface by ~900 K.

(4) $B_{10}H_{14}$ decomposes on the Si(111) surface by first breaking the B-H-B bonds.

(5) Subsequent heating promotes bulk boron diffusion and produces an ordered Si(111)-B($\sqrt{3}\times\sqrt{3}$)R30° surface with an upper limit of 1/3 ML boron occupying the subsurface, substitutional sites in

14

the first silicon bilayer.

(6) The sharpness of this boron δ-doped layer is largely limited
     by the high temperature required to form this ordered
     structure.

(7) In the near surface region ($\sim 10^2$ Å), a typical effective
     carrier hole concentration of $\sim 2 \times 10^{19}$ cm^{-3} has been deduced
     from the surface plasmon frequency (after correction for
     damping), ω_{sp}, based on HREELS measurements.

Acknowledgements

References

[1]   R. L. Headrick, I. K. Robinson, E. Vlieg and L. C. Feldman, Phys. Rev. Lett. 63 (1989) 1253.

[2]   P. Bedrossian, R. D. Mead, K. Mortensen, D. M. Chen, J. A. Golovchenko and D. Vanderbilt, Phys. Rev. Lett. 63 (1989) 1257.

[3]   I.-W. Lyo, E. Kaxiras and Ph. Avouris, Phys. Rev. Lett. 63 (1989) 1261.

[4]   Ph. Avouris, I.-W. Lyo, F. Boszo and E. Kaxiras, J. Vac. Sci. Technol. A8 (1990) 3405.

[5]   P. J. Chen, M. L. Colaianni and J. T. Yates, Jr., J. Appl. Phys. 70 (1991) 2954.

[6]   F. Bozso and Ph. Avouris, Phys. Rev. B44 (1991) 9129.

[7]   R. L. Headrick, B. E. Weir, A. F. Levi, D. J. Eaglesham and L. C. Feldman, Appl. Phys. Lett. 57 (1990) 2779.

[8]   A. B. McLean, L. J. Terminello and F. J. Himpsel, Phys. Rev. B41 (1990) 7694.

[9]   R. L. Headrick, B. E. Weir, J. Bevk, B. S. Freer, D. J. Eaglesham and L. C. Feldman, Phys. Rev. Lett. 65 (1990) 1128.

[10] R. L. Headrick, B. E. Weir, A. F. J. Levi, B. Freer, J. Bevk and L. C. Feldman, J. Vac. Sci. Technol. A9 (1991) 2269.

[11] Z. Zhang, Y.-G. Kim, P. A. Dowben and J. T. Spencer, in Mat. Res. Soc. Symp. Proc. v. 131, edited by M. E. Gross, J. M. Jasinski and J. T. Yates, Jr. (1989) 401.

[12] Y. G. Kim, P. A. Dowben, J. T. Spencer and G. O. Ramseyer, J. Vac. Sci. Technol. A7 (1989) 2796.

[13] R. A. Rosenberg, F. K. Perkins, D. C. Mancini, G. R. Harp, B. P. Tonner, S. Lee and P. A. Dowben, Appl. Phys. Lett. 58 (1991) 607; F. Keith, R. A. Rosenberg, S. Lee and P. A. Dowben, J. Appl. Phys. 69 (1991) 4103.

[14] M. L. Yu, D. J. Vitkavage and B. S. Meyerson, J. Appl. Phys. 59 (1986) 4032.

[15] G. Dujardin, R. E. Walkup and Ph. Avouris, Science 255 (1992) 1232.

[16] M. L. Colaianni, P. J. Chen and J. T. Yates, Jr., J. Chem. Phys. in press.

[17] The mass spectrum of $B_{10}H_{14}$ has been obtained with our QMS in the mass range of 1-135 amu at an electron impact energy of 70 eV. It is in excellent agreement with the literature; see I. Shapiro et al. in "Borax to Boranes, Advances in Chemistry Series No.32", R. F. Gould ed., American Chemical Society, Washington D.C. (1961), pg. 129.

[18] F. J. Himpsel, F. R. McFeely, A. Taleb-Ibrahimi and J. A. Yarmoff, Phys. Rev. B38 (1988) 6084. An extrapolated value of 7 Å is used as the escape depth for the 179 eV B(KLL) Auger electrons. The relaxed B position is 2.32 Å below the Si surface according to Refs. 1-3.

[19] R. M. Adams, ed.,"Boron, Metallo-Boron Compounds and Boranes", Interscience, New York (1964).

[20] J. J. Miller and M. F. Hawthorne, J. Am. Chem. Soc. 81 (1959) 4501.

[21] P. J. Chen, M. L. Colaianni, R. M. Wallace and J. T. Yates, Jr., Surf. Sci. 244 (1991) 177.

[22] S. M. Sze, "Semiconductor Devices", Wiley, New York (1985).

[23] H. Ibach and D. L. Mills "Electron Energy Loss Spectroscopy and Surface Vibrations", Academic Press, New York (1982).

[24] Y. Meng, J. R. Anderson, J. C. Hermanson and G. J. Lapeyre, Phys. Rev. B44 (1991) 4040.

[25] J. E. Rowe, R. A. Malic, E. E. Chaban, R. L. Headrick and L. C. Feldman, J. Electon Spect. Rel. Phenomn. 54/55 (1990) 1115.

[26] J. E. Rowe, private communication.

[27] A reliable estimate of B diffusion depth can be obtained from an extensive body of literature on B diffusion in Si. For the B concentration of interest here, the diffusion is extrinsic, i.e., the diffusion coefficient varies as a function of B concentration (Ref.22, pg.391). Applying the proper model yields a diffusion depth of $\sim 10^3$ Å after annealing at 1273 K for 300 seconds. This value is in good agreement with SIMS measurements of the B concentration profile on the Si(111) crystals.

[28] P. J. Chen, J. E. Rowe and J. T. Yates, Jr., to be submitted.

[29] P. J. Chen, M. L. Colaianni and J. T. Yates, Jr., to be submitted.

Figure Captions

Figure 1. (a) HREEL spectra of $B_{10}H_{14}$ condensed on Si(111)-(7x7) surface at 100 K. The spectra were taken at a primary electron energy E_p=6.1 eV. The Auger ratio B(179 eV)/Si(92 eV) indicates the relative surface coverage resulting from varying $B_{10}H_{14}$ exposures. The corresponding surface coverages are indicated in parentheses (1 ML=7.8×10^{14} $B_{10}H_{14}$ molecules cm^{-2}); (b) Schematic representation of the infrared absorption of $B_{10}H_{14}$ based on Ref.19.

Figure 2. Schematic molecular structure of decaborane ($B_{10}H_{14}$). In addition to the conventional two-center B-H and B-B bonding, there also exists the (electron-deficient) three-center bonding in the form of B-H-B and B-B-B. There are a total of four H atoms in a bridge-bonded B-H-B configuration and ten H atoms in the terminal B-H configuration.

Figure 3. Temperature programmed desorption of H_2 (m/e=2) from a Si(111)-(7x7) surface after ~2 L $B_{10}H_{14}$ exposure. The heating rate was 1 K/sec.

Figure 4. HREELS measurements of the thermal behavior of the $B_{10}H_{14}$ overlayer. The initial $B_{10}H_{14}$ surface coverage was 0.35 ML at 100 K. Each spectrum was taken after heating to specified temperatures, and cooling back to 100 K.
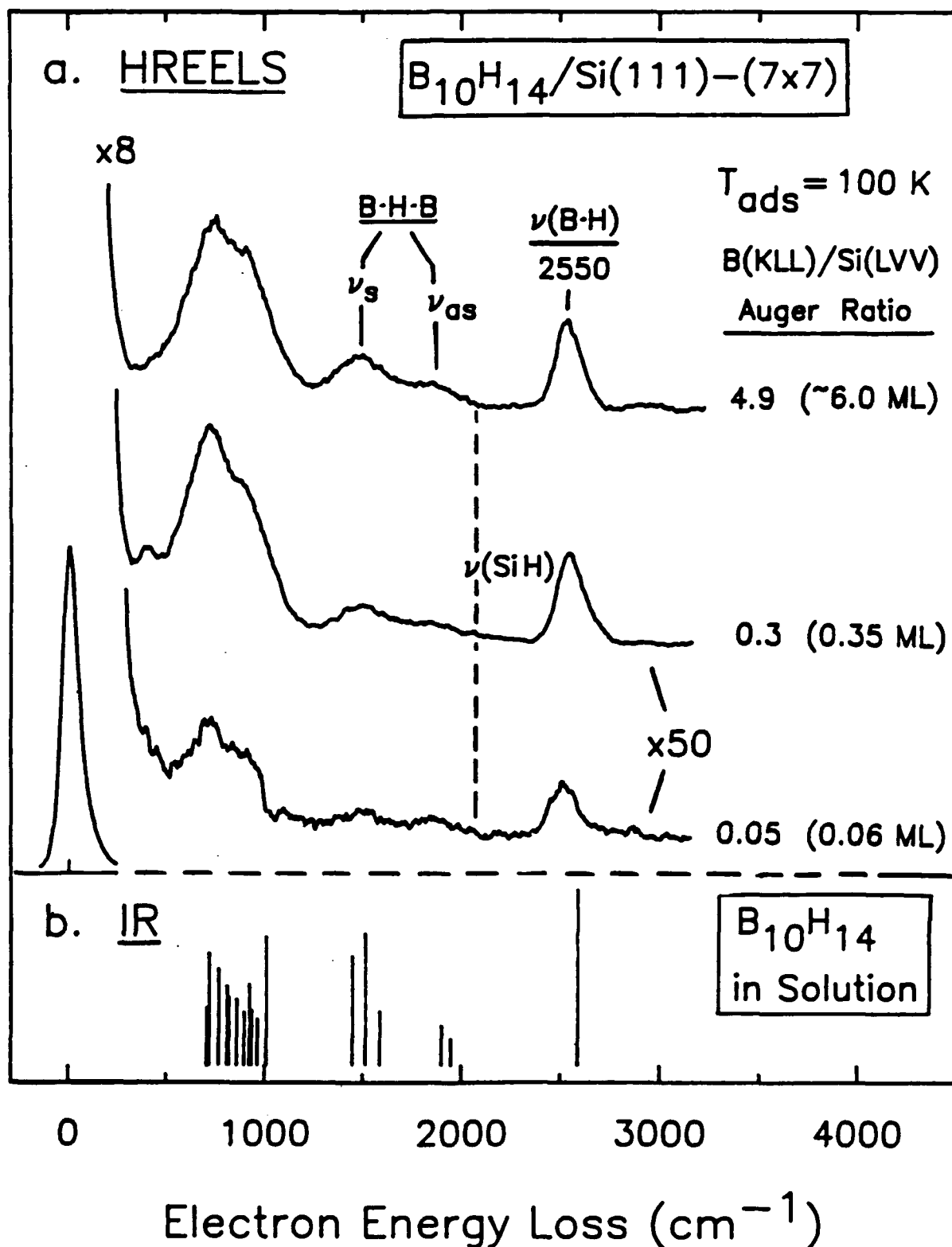
Figure 5. (a) The structure of the $Si(111)-B(\sqrt{3}x\sqrt{3})R30°$ surface with the $(\sqrt{3}x\sqrt{3})R30°$ unit cell outlined. The B atoms occupy the subsurface, substitutional S_5 sites in the first Si bilayer underneath atop Si atoms. (b) HREEL spectrum taken from a well-ordered $Si(111)-B(\sqrt{3}x\sqrt{3})R30°$ surface at 100 K with a primary electron energy $E_p=3.2$ eV. The peak position of the surface hole-plasmon loss, ω_{pp}, is at 505 cm^{-1}. The loss peak belonging to the localized B-Si optical phonon mode is at 770 cm^{-1}. The inset shows schematically the approximate composition of the surface (on an expanded scale) and the bulk region of the boron-treated Si(111) crystal.

Table I

Typical B-H Bond Infrared Absorption Frequencies [19]

Mode	Frequency (cm^{-1})
BH (terminal) stretch	2530 - 2590
BH (bridge) sym. breathing	1915
asym. breathing	1602
BH in-plane bend	1105 - 1114

Vibrational Spectra of Decaborane on Si(111)−(7x7

a. HREELS

$B_{10}H_{14}/Si(111)-(7x7)$

x8

B·H·B

ν_s ν_{as}

$\nu(B·H)$
2550

$T_{ads} = 100$ K

B(KLL)/Si(LVV)

Auger Ratio

4.9 (~6.0 ML)

$\nu(SiH)$

0.3 (0.35 ML)

x50

0.05 (0.06 ML)

b. IR

$B_{10}H_{14}$
in Solution

0   1000   2000   3000   4000

Electron Energy Loss (cm^{-1})

Chen,
Colaianni,
Yates

Molecular Structure of Decaborane
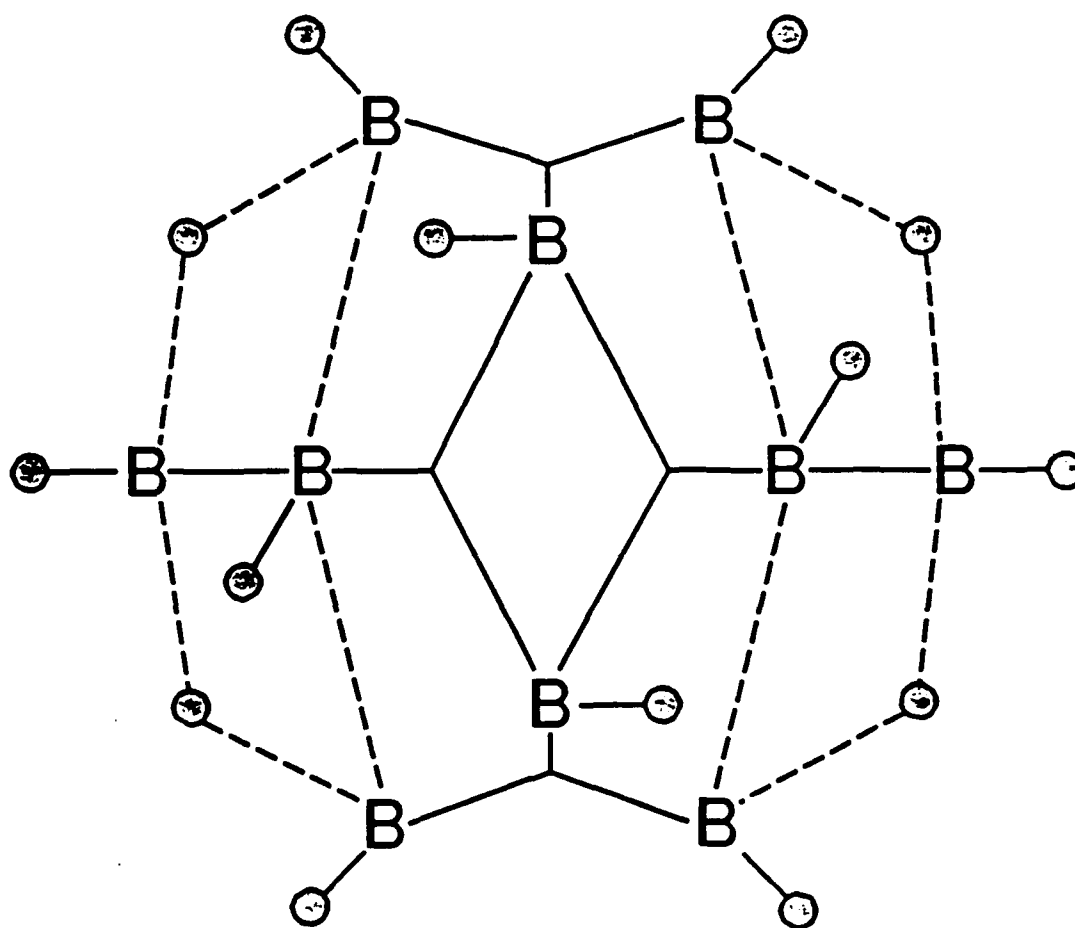
H$_2$ Desorption from B$_{10}$H$_{14}$ on Si(111)

dT/dt = 1 K/sec

1.5x10^{-9} A

Mass 2 Intensity (arb. unit)

Temperature (K)
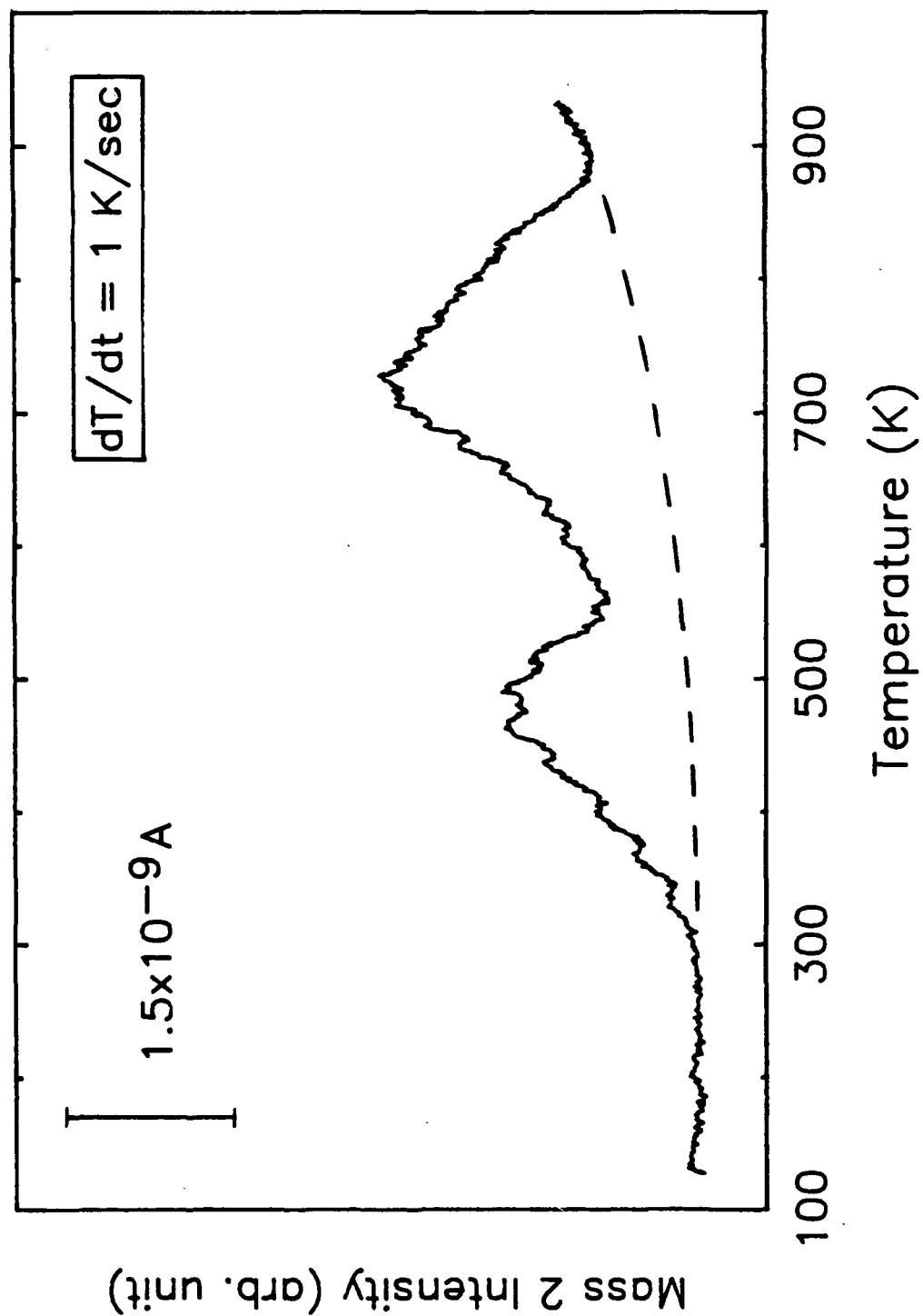
Thermal Behavior of Decaborane Overlayer On Si(111)–(7x7) Studied by HREELS

Chen, Colaianni, Yates

Figure 4
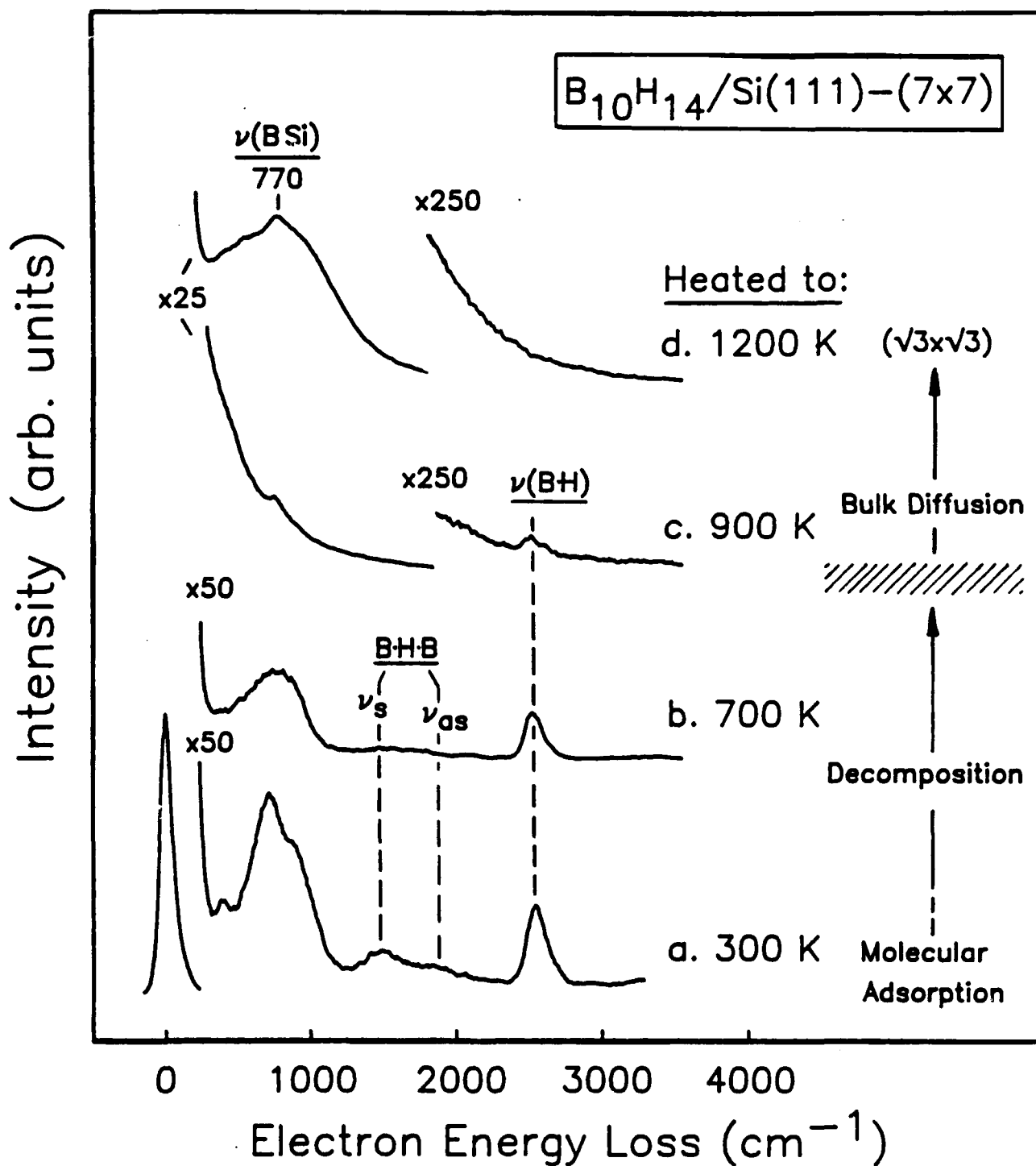
Structure of Si(111)–B(√3x√3)R30° Surface and HREELS Studies

a.

$(\bar{1}10)$

$(11\bar{2})$

⊘ = Atop Si Atom

○ = Lattice Si Atom

● = B Atom

(111)

$(11\bar{2})$

b.

$E_p = 3.2$ eV
$T = 100$ K

ω_{pp} $\dfrac{\nu(B-Si)}{770}$

$n_B = 7 \times 10^{21}$ cm^{-3}

0

$n_B \approx 2 \times 10^{19}$ cm^{-3}

100 Å

x20

Electron Energy Loss (cm^{-1})
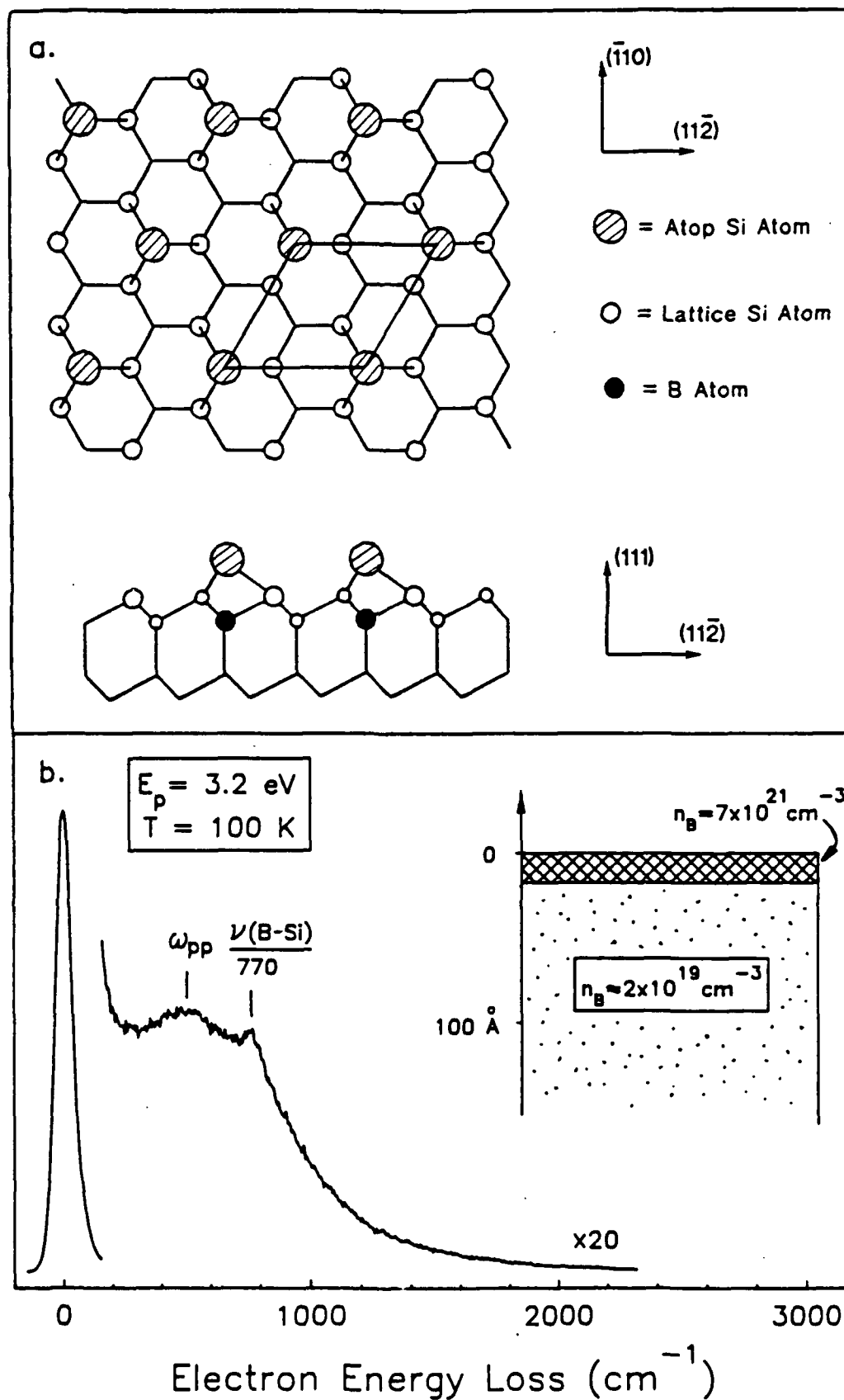
ALE Contractor Distribution List	# Copies
D.T.I.C. Bldg # 5, Cameron Station Alexandria, VA 22314	12
Dr. Andrew Freedman Aerodyne Research, Inc. 45 Manning Road Billerica, MA 01821 Tel: (508) 663-9500 FAX: (508) 663-4918 e-mail: aerodyn@mitvma.mit.edu	1
Dr. Asif Kahn APA Optics 2950 NE 84th Lane Blaine, MN 55434 Tel: (612) 784-4995 FAX: (612) 784-2038 e-mail: 70702.2032@compuserve.com	1
Dr. Duncan Brown Advanced Technology Materials, Inc 7 Commerce Drive Danbury, CT 06810 Tel: (203) 794-1100 FAX: (203) 792-8040	1
Dr. Peter Norris EMCORE Corp. 35 Elizabeth Ave. Somerset, NJ 08873 Tel: (201) 271-9090	1
Prof. Joe Greene Dept. of Materials Science and Engineering University of Illinois 1101 W. Springfield Ave. Urbana, IL 61801 Tel: (217) 333-0747	1
Dr. T. P. Smith IBM T.J. Watson Research Center P. O. Box 218, Route 134 Yorktown Heights, NY 10598 e-mail: trey@ibm.com	1
Prof. Robert F. Davis N.C.S.U. Box 7907	1

Raleigh, NC 27695-7907
Tel: (919) 515-2377/3272
FAX: (919) 515-3419
e-mail: davis@mte.ncsu.edu

Prof. Salah Bedair   1
Department of Electrical Engineering
N.C.S.U.; Box
Raleigh, NC 27695
Tel: (919) 515-2336
e-mail: jll@@ecegrad.ncsu.edu

Max N. Yoder   1
ONR Code 1114
Arlington, VA 22217
Tel: (703) 696-4218
FAXes (703) 696-2611/3945/5383
e-mail: yoder@charm.isi.edu

Dr. A. M. Goodman   1
ONR, Code 1114
Arlington, VA 22217
Tel: (703) 696-4218
FAXes (703) 696-2611/3945/5383
e-mail: goodman@ocnr-hq.navy.mil

Dr. J. Pazik   1
ONR Code 1113
Arlington, VA 22217
Tel: (703) 696-4410
FAXes (703) 696-2611/3945/5383
e-mail: pazik@ocnr-hq.navy.mil
        pazik%estd.decnet@ccf.nrl.navy.mil

Prof. J. T. Yates, Jr.   1
Dept. of Chemistry
Surface Science Ctr.
University of Pittsburgh
Pittsburgh, PA 15260
Tel: (412) 624-8320
FAX: (412) 624-8552
e-mail: yates@vms.cis.pitt.edu

Robert J. Markunas, R.A. Rudder   1
Research Triangle Institute; Box 12194
Research Triangle Park, NC 27709-2194
Tel: (919) 541-6153
FAX: (919) 541-6515
e-mail: rjmk@rti.rti.org

Professor Mark P. D'Evelyn   1
William Marsh Rice University
Dept. of Chemistry
P.O. Box 1892
Houston, TX 77251
Tel: (713) 527-8101, ext. 3468
FAX: (713) 285-5155
e-mail: mpdev@@langmuir.rice.edu

Dr. Howard K. Schmidt   1
Schmidt Instruments, Inc.
2476 Bolsover, Suite 234
Houston, TX 770054
Tel: (713) 529-9040

FAX: (713) 529-1147
e-mail: hksionwk@ricevml.rice.edu

Prof. A. F. Tasch   1
Dept. of Electrical Engr. & Computer Science
Engineering Science Bldg.
University of Texas at Austin
Austin, TX 78712
Tel:
FAX:
e-mail: tasch@roz.ece.utexas.edu

Prof. Charles Tu   1
Dept of Electrical & Computer Engr.
UCSD
LaJolla, CA
Tel: (619) 534-4687
FAX: (619) 534-2486
e-mail: cwt@celece.ucsd.edu

Prof. John E. Crowell   1
Department of Chemistry
University of California at San Diego
LaJolla, CA
Tel: (619) 534-5441
FAX: (619) 534-0058
email: jcrowell@ucsd.edu

Prof. P. Daniel Dapkus   1
University of Southern California
University Park
Los Angeles, CA   90089-1147
e-mail: dapkus@mizar.usc.edu
Tel: (213) 740-4414
FAX: (213) 740-8684